

1

2 ENERGY CORRELATORS AS A PROBE OF THE HARD PROCESS IN RUN 24 $p - p$
3 COLLISIONS AT $\sqrt{s} = 200 \text{ GeV}$ WITH THE sPHENIX DETECTOR AT RHIC

4 by

5 SKADI KURT GROSSBERNDT

6 A dissertation submitted to the Graduate Faculty in Physics in partial fulfillment of the
7 requirements for the degree of Doctor of Philosophy, The City University of New York

8 2025

9

10

© 2025

11

SKADI KURT GROSSBERNDT

12

All Rights Reserved

- ¹³ This manuscript has been read and accepted by the Graduate Faculty in Physics in
¹⁴ satisfaction of the dissertation requirement for the degree of Doctor of Philosophy.

Professor Stefan Bathe

Date Chair of Examining Committee

15

Professor Daniel Kabat

Date Executive Officer

Professor Adrian Dimitru

Professor Raghav Kunnawalkam Elayavalli

16

Professor Jamal Jallian-Marian

Professor Miguel Castro Nunes Fiolhais

Supervisory Committee

17

Abstract

ENERGY CORRELATORS AS A PROBE OF THE HARD PROCESS IN RUN 24 $p - p$

COLLISIONS AT $\sqrt{s} = 200$ GeV WITH THE SPHENIX DETECTOR AT RHIC

by

SKADI K GROSSBERNDT

²³ Adviser: Professor Stefan Bathe

²⁴ This dissertation consists of three parts in addition to a literature review establishing the
²⁵ state of the art of jet physics and the Energy-Energy correlator at high energies...

26 Part 1: Hardware This part discusses the physical hardware used to make the measure-
27 ments of the energy in the jets created by the proton-proton collisions. This part contains a
28 discussion of the sPHENIX detector and an in-depth look at the relevant susbsystems for the
29 meausements in this analysis. In addition, the Monte Carlo methods and models to discern
30 the expected respnse and calibrate the detector are discussed in detail, with both subparts
31 coming together in a disucssion of backgrounds and error calculation in general and for the
32 observables at hand.

³³ **Part 2: Technicalities** This part builds from first principles up to the jet measurement
³⁴ in a theoretical light, and then discusses the additional computational techniques on display
³⁵ that will provide the bridge between the theory of these observables and the practical ap-
³⁶ plication to sPHENIX. This part contains a chapter that is a pared down discussion of a
³⁷ midstream paper proposed as part of the thesis process that establishes the safety of this
³⁸ observable against jet finding choices.

³⁹ **Part 3: Experimental Output** This part is the meat and potatoes of the dissertation,
⁴⁰ discussing results from the experiment and the analysis in light of the previous parts and
⁴¹ comparing to the world results from related systems.

⁴² Contents

⁴³ 1 Literature Review	¹
44 1.1 Jets Definitions	2
45 1.1.1 Jet Reconstruction Algorithms	2
46 1.1.2 Quark and Gluon Jets	2
47 1.2 Jet Substructure Measurements	3
48 1.3 N-Point Energy Correlator	3
⁴⁹ I Hardware: The Detector and Simulations	⁴
⁵⁰ 2 The sPHENIX detector	⁵
51 2.1 Calorimetry	6
52 2.1.1 Analog Digital Converters and Data Acquisition	6
53 2.1.2 Hadronic Calorimeters	8
54 2.1.3 Electromagnetic Calorimeter	9
55 2.1.4 Zero Degree Calorimeter	10
56 2.2 Tracking	10
57 2.2.1 INTT	11
58 2.2.2 Micromegas Vertex Detector	11
59 2.2.3 Time Projection Chamber	11

<i>CONTENTS</i>	vii
60 2.2.4 TPC Outer Tracker	11
61 2.3 Event Characterization	11
62 2.3.1 sPhenix Event Plane Detector	11
63 2.3.2 Minimum Bias Detector	11
64 2.4 Triggers	11
65 3 Monte Carlo Simulations	12
66 4 Determining Backgrounds and Errors	13
67 II Technicalities: The finer points of theory and computing	14
68 5 The Energy Correlator and the primary vertex	15
69 6 Jets in Vacuum and the PDF	16
70 6.1 Jet Identification Algorithms	16
71 7 So exactly how intelligent is AI	17
72 8 Proof Solving and Validation as Quality Control Mechanisms	18
73 III Experimental Output: The Main Event	19
74 9 So is sPHENIX actually working?	20
75 10 Measuring the Energy Correlator	21
76 11 The Power of the ENC: α_s at the few GeV scale	22
77 12 Event-by-Event distinguishing	23

78	13 Comparison is the Theft of Joy: What does the LHC say, and how about STAR?	24
80	14 Entanglement and other Lofty Goals	25
81	IV Wrapping it all up	26
82	15 Observable prospects for Run 25 and the EIC	27
83	16 Remaining Questions	28
84	17 Implementation and application for the remaining sPHENIX data	29

⁸⁵ **List of Tables**

⁸⁶ **List of Figures**

⁸⁷ 2.1	The sPHENIX detector. The Zero Degree Calorimeter is not picutred but is located further along the beam pipe.	6
⁸⁸ 2.2	Top: Persistence Waveform. Bottom: Energy distribution averaged across 10^5 events	9
⁸⁹		
⁹⁰		

₉₁ Chapter 1

₉₂ Literature Review

⁹³ 1.1 Jets Definitions

⁹⁴ The study of Quantum Chromodynamics in high energy collisions, such as those at the
⁹⁵ Relativistic Heavy Ion Collider or the Large Hadron Collider, is often carried out through
⁹⁶ investigation of the kinematics of jets. Jets, as objects, sit in the boundary between experiment
⁹⁷ and theory, being an experimental signature corresponding to final states of quarks and
⁹⁸ gluons produced in collisions. Jets are a cluster of final state particles that result from the
⁹⁹ showering and hadronization of the initial parton, that are identified in experiment through
¹⁰⁰ use of one of the multiple jet reconstruction algorithms.

¹⁰¹ 1.1.1 Jet Reconstruction Algorithms

¹⁰² In Ryan Atkin's paper *Review of jet reconstruction algorithms* [1], Atkin provides an overview
¹⁰³ of the standard algorithms with a focus on practical implementation for experimental usage.
¹⁰⁴ Atkin discusses a number of algorithms that fall into two categories: Cone based and Se-
¹⁰⁵ quential Clustering

¹⁰⁶ Cone Methods

¹⁰⁷ In Atkin's paper, Atkin discusses two iterative cone procedures—Iterative Cone with Pro-
¹⁰⁸ gressive Removal and with Split Merge—and one more modern cone method, Seedless Infrared
¹⁰⁹ Safe Cone. These iterative cone procedures are described as simple to implement in an ex-
¹¹⁰ perimental context, however, they both suffer deficiencies from a theoretical perspective as
¹¹¹ they fail to be IRC safe [1] [2].

¹¹² 1.1.2 Quark and Gluon Jets

¹¹³ In their paper *An Operational Definition of Quark and Gluon Jets* [3] Kimiske, Metodiev
¹¹⁴ and Thaler present a theoretical definition of jet flavor with an eye towards application

at colliders. They aim to present a precise and practical definition of jet flavor at the hadron level, thus allowing for direct measurement from collider experiments rather than a measurement by proxy. While the gluon or quark jet is well defined at the level of the hard scattering, corresponding to an initiating parton of the primary vertex [4] [5]. Experimentally, there is significant interest in being able to discriminate quark and gluon jets in searches for BSM physics, searches for Dark Matter, in jet substructure analysis, in QGP physics and in understanding the processes of hadronization [6][7][8]]. The determination of relative populations of quark and gluon jets in a dijet sample is one of the primary tasks of this thesis and will be discussed at length in chapters 11 and 12.

Kimiske et al. begin their

1.2 Jet Substructure Measurements

1.3 N-Point Energy Correlator

127

Part I

128

Hardware: The Detector and Simulations

129

¹³⁰

Chapter 2

¹³¹

The sPHENIX detector

¹³² The sPHENIX detector is part of the Relativistic Heavy Ion Collider (RHIC) complex at
¹³³ Brookhaven National Laboratories (BNL) in Upton, New York. RHIC is one of two major
¹³⁴ circular particle colliders in the world, the other of which is the Large Hadron Collider at
¹³⁵ CERN in Geneva, Switzerland. Over the course of the sPHENIX experiment which will
¹³⁶ run from run 23 until RHIC ceases operations after run 25, RHIC will be colliding gold
¹³⁷ nuclei and protons with run 23 having been dedicated to commissioning Au+Au running,
¹³⁸ run 24 dedicated to p+p with three weeks of Au+Au for further tracking commissioning
¹³⁹ and run 25 dedicated to physics running in Au+Au collisions. RHIC runs with a center of
¹⁴⁰ mass energy of $\sqrt{s} = 200\text{GeV}$ for both protons and gold, and additionally is the sole col-
¹⁴¹ linder that collides polarized protons, which allows for more in depth studies of spin physics.
¹⁴² At RHIC, sPHENIX's forerunner, the Pioneering High Energy Nuclear Interaction eXper-
¹⁴³ iment (PHENIX), performed the first measurement of the Quark Gluon Plasma droplets
¹⁴⁴ [QGP droplets] in nuclei-nuclei collisions.

¹⁴⁵ sPHENIX is designed to offer significant upgrades to PHENIX, specifically providing in-
¹⁴⁶ creased coverage with hadronic and electromagnetic calorimeters, increasing effectiveness in
¹⁴⁷ studies of jets and heavy flavor at mid-to-high Bjorken x [sPHENIX TDR][sPHENIX whitepaper][sPHENIX paper]

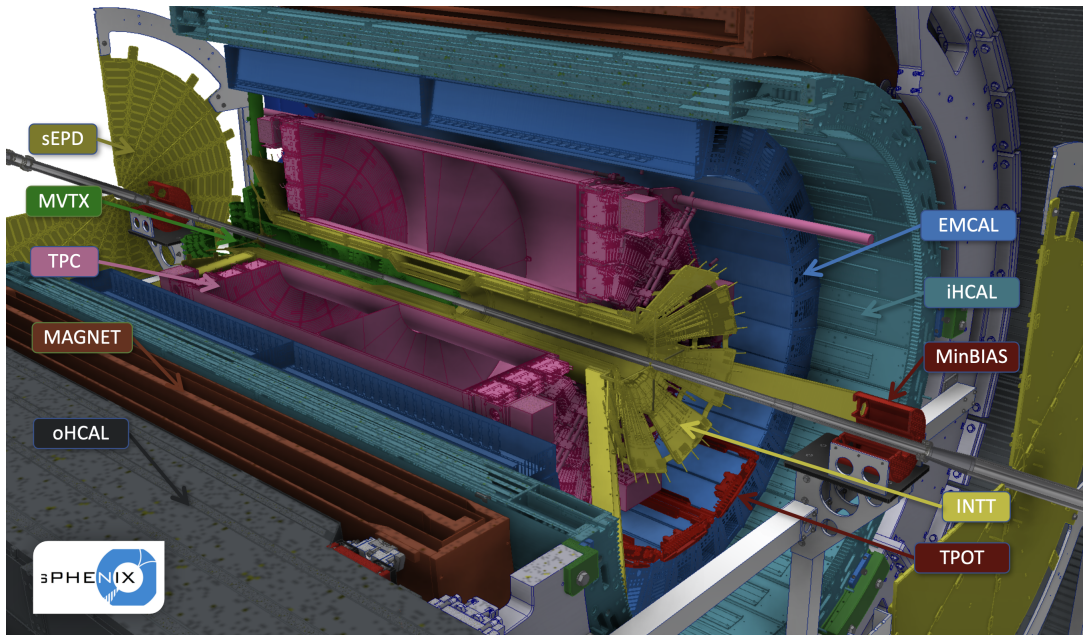


Figure 2.1: The sPHENIX detector. The Zero Degree Calorimeter is not pictured but is located further along the beam pipe.

₁₄₈ Broadly, sPHENIX can be broken into three categories of subsystem: Calorimeters, Tracking
₁₄₉ and Event characterization. sPHENIX is constructed around a 1.5 Tesla superconducting
₁₅₀ magnet, cooled by liquid helium, which was previously used on the BABAR experiment at
₁₅₁ SLAC.

₁₅₂ 2.1 Calorimetry

₁₅₃ 2.1.1 Analog Digital Converters and Data Acquisition

₁₅₄ Beyond the purposes and hardware of the detector itself, one can further characterize the
₁₅₅ subsystems of sPHENIX into streaming readout and non-streaming detectors, broadly dis-
₁₅₆ tinguishing the tracking detectors from other subsystems. The non-streaming detectors all
₁₅₇ use a common data acquisition pipeline and data format. These detectors are readout to
₁₅₈ analog digital converters boards with 64 channels each, which are then grouped into sets

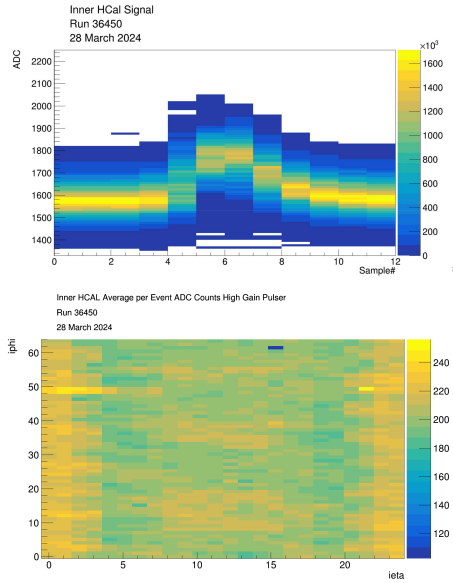
159 of 3 called an "XMIT" group, which is then read to the data format as a "packet" of 192
160 channels. Each packet is transmitted from the detector to the computing center on a seper-
161 ate fiber optic cable that is then read into a digitizer which forms groups of (at most) eight
162 packets that are then assigned to individual data acquisition servers. The digitizing process
163 allows for readback into the detector through a global trigger and timing module, where
164 each DAQ server, can issue commands and readback to an event building logic that will then
165 flow back to the detector controlling the same XMIT groups. Each set of (at most) 4 XMIT
166 groups is arranged into a crate with a single crate controller that receives trigger and timing
167 information distributed via a global timing and level 1 trigger module (GL1/GTM) that is
168 then processed through a clockmaster for each digitizer rack, which will hold between 1 and
169 4 crates, depending of the needs of the subsystem. The data read out to each DAQ server
170 is then stored in the "Porschke Raq Data Format" or prdf file that provides an event struc-
171 ture consisting of a header with some identifying information and separate headers for each
172 packet, but is otherwise comprehensible as an ASCII file. This event structure allows for easy
173 offline combination of events across the calorimeters while keeping individual file size buffers
174 relatively small, as each packet has timing information along with an event number relative
175 to the run that is inherited from the timing module. This DAQ configuration is currently
176 used for the calorimeters, the event plane detector and the minimum bias detector, which
177 allows for faster event building to verify data quality and alignment. The tracking detectors
178 utilize a streaming readout format that creates event pools that are then associated with
179 beam crossing timings provided by the RHIC clock and can be matched onto the GTM tim-
180 ing in offline analysis. This process is slow, and currently under development, hence there is
181 a lack of tracking data presently available

2.1.2 Hadronic Calorimeters

sPHENIX's power in jet physics comes in large part from its calorimeter systems, including two separate hadronic calorimeters. The outer and inner hadronic calorimeter (OHCAL and IHCal respectively) are both divided into 24 bins in η with coverage of $|\eta| \leq 1.1$ and full φ coverage with 64 bins in φ , grouped in φ into 32 sectors in each calorimeter. Each hadronic calorimeter therefore has tower size of $\delta\eta = 0.092$ and $\delta\varphi = 0.098$. The outer hadronic calorimeter is constructed of steel and sits outside of the magnet, with inner radius of $r = 1.82$ m and outer radius of $r = 2.69$ m. The inner hadronic calorimeter is constructed of aluminum and sits just inside the magnet, with inner radius of $r = 1/16$ m and outer radius of $r = 1.37$ m. Each tower corresponds to a readout board that sums readout from four scintillator paddles embeded into the calorimeter as show in fig. ???. These interface boards form a single readout channel, and can be individually teste via a pulser system that injects charge into the interface board testing readback independent of scintillator response, and LED system that injects a fixed pulse of light into the scintilators to test behavior of the Silicon Photomultipliers (SiPMs). Output of each of these systems is shown in fig 2.2

Calibration

The hadronic calorimeters were intially calibrated through use of cosmic ray muons, matching the spectra to Monte Carlo generated through EcoMug and GEANT4 [**HCal·Calib**]. This calibration is updated through out the run via continued cosmic ray studies in between physics data taking in addition to ongoing work on in-situ calibrations using tower-slope methods [**tower·slope·hcal**]. These calibrations have yeilded an average conversion factor for the OHCAL of and the IHCal of



(a) Charge Injection Pulse. This system allows for direct testing of electronics without detector response

(b) LED pulse. This allows for testing of the full readback system and light response

Figure 2.2: Top: Persistence Waveform. Bottom: Energy distribution averaged across 10^5 events

2.1.3 Electromagnetic Calorimeter

Moving in one layer from the hadronic calorimeter, the Electromagnetic Calorimeter (EMCal) has the same coverage in $\eta - \varphi$ space, but has 16 times as many towers with 96 bins in η and 256 bins in φ . The EMCal is constructed of blocks of tungsten with embedded scintillation fibers, and had inner radius $r = 0.9$ m and outer radius of $r = 1.16$ m. Similarly to the HCals, the EMCal is also equipped with a pulser and LED, although the increased number of towers and higher variability in response requires that different pulse widths be used for separate sets of towers to prevent saturation and clipping on the LED pulse.

Calibration

The EMCal was calibrated to the π^0 mass through the $\pi^0 \rightarrow \gamma\gamma$ decay channel with additional corrections applied via the tower slope. The mean m_{π^0} and width are used as quality

215 assurance plots to monitor radiation damage to the EMCal on an ongoing basis.

216 2.1.4 Zero Degree Calorimeter

217 The Zero Degree Calorimeter (ZDC) is a small transverse energy hadron detector that po-
218 sitioned outside of the experiment hall, in the tunnels along the beam pipe, 18 m from the
219 interaction point on both side. The ZDC is used to detect spectator neutrons to allow for the
220 calculation of multiplicity and event geometry, making it an overlapping detector between
221 the calorimeters and the event characterization [9]. In addition, the ZDC provides a good
222 proxy for total collision rates, useful for both real time monitoring of beam conditions and
223 The sPHENIX ZDC is one of two detectors that was preserved from PHENIX, with minor
224 repairs and upgrades to improve running. In pp collisions, the ZDC provides additional
225 utility as a spin momentum detector that allows for measurement of the spin patterns of the
226 RHIC beam through the Vernier Scan. This functionality is pivotal for the development
227 of sPHENIX’s spin physics program in pp and its extensions into the continuing physics
228 goals at the Electron Ion Collider (EIC)[9]. For the purposes of this work, the ZDC is not
229 utilized for either spin physics or trigger capabilities and serves primarily to help establish
230 cross-sections for error determination. While this work does not dive into the subject of
231 spin dependence, such topics are a natural extension and present an interesting avenue for
232 future studies in this vein to be done with the sPHENIX Run 24 data set.

233 2.2 Tracking

234 The sPHENIX tracking system consists of the Silicon vertexing detectors and the gas based
235 trackers.

²³⁶ **2.2.1 INTT**

²³⁷ **2.2.2 Micromegas Vertex Detector**

²³⁸ The Micromegas Vertex detector (MVTX) is a silicon based vertexing detector based on a
²³⁹ similar system at the ALICE experiment of the Large Hadron Collider (LHC).

²⁴⁰ **2.2.3 Time Projection Chamber**

²⁴¹ The Time Projection Chamber (TPC)

²⁴² **2.2.4 TPC Outer Tracker**

²⁴³ The TPC Outer Tracker (TPOT) was designed as a minimal add-on to improve tracking
²⁴⁴ efficiency and resolution by providing additional track points.

²⁴⁵ **2.3 Event Characterization**

²⁴⁶ **2.3.1 sPhenix Event Plane Detector**

²⁴⁷ **2.3.2 Minimum Bias Detector**

²⁴⁸ The sPHENIX Minimum Bias Detector (MBD) is the other detector preserved from PHENIX,
²⁴⁹ when it was called the Beam-Beam Counter (BBC). This detector is situated

²⁵⁰ **2.4 Triggers**

²⁵¹ The sPHENIX detector has a number of triggers at its disposal to allow for online event type
²⁵² selections for the triggered readout system: the EMCal, the HCals, the ZDC, the MBD, the
²⁵³ sEPD and—for run 2024—the TPC. Starting in run 2024, available triggers are Minimum Bias

²⁵⁴ **Chapter 3**

²⁵⁵ **Monte Carlo Simulations**

²⁵⁶ We have some of them, there is some data from the 2 and three point energy correlator, and
²⁵⁷ its important for training of our discriminator

²⁵⁸ Chapter 4

²⁵⁹ Determining Backgrounds and Errors

260

Part II

261

**Technicalities: The finer points of
theory and computing**

262

263 **Chapter 5**

264 **The Energy Correlator and the
primary vertex**

266 So the energy correlator allows a look back, I guess that's the relevant bit? Point being, if
267 the jet points back to the primary vertex, the share of the energy between the jets and the
268 composition of those jets is directly determined by the $2 \rightarrow 2$ scattering and is thus sensitive
269 to the parton distribution functions of the beam particles. Starting from the definition of
270 the energy correlator given in [10]:

$$\mathcal{E}_N = \int \frac{d\Omega}{2} \int d\vec{n}_{12} \frac{\langle \varepsilon(\vec{n}_1) \dots \varepsilon(\vec{n}_2) \rangle}{Q^2} \delta(\vec{n}_1 \cdot \vec{n}_2 - 2|\vec{n}_1| |\vec{n}_2| \cos \theta) \quad (5.1)$$

271 **Chapter 6**

272 **Jets in Vacuum and the PDF**

273 **6.1 Jet Identification Algorithms**

274 As discussed in chapter 1, there are a variety of jet finding algorithms that prioritize different
275 theoretical aspects of the underlying physics while being experimentally realizable [11] [1].

276 In general, a jet identification algorithm needs to be IRC safe. That is, the jet object
277 needs to display invariance in the Infrared (IR) and Collinear regimes, managing real-virtual
278 cancellation and keeping results meaningful for emission and splitting respectively.

²⁷⁹ Chapter 7

²⁸⁰ So exactly how intelligent is AI

²⁸¹ Chapter 8

²⁸² Proof Solving and Validation as
²⁸³ Quality Control Mechanisms

284

Part III

285

Experimental Output: The Main Event

286

287 Chapter 9

288 So is sPHENIX actually working?

²⁸⁹ Chapter 10

²⁹⁰ Measuring the Energy Correlator

²⁹¹ Chapter 11

²⁹² The Power of the ENC: α_s at the few

²⁹³ GeV scale

²⁹⁴ Chapter 12

²⁹⁵ Event-by-Event distinguishing

²⁹⁶ Chapter 13

²⁹⁷ Comparison is the Theft of Joy: What
²⁹⁸ does the LHC say, and how about
²⁹⁹ STAR?

³⁰⁰ Chapter 14

³⁰¹ Entanglement and other Lofty Goals

302

Part IV

303

Wrapping it all up

³⁰⁴ Chapter 15

³⁰⁵ Observable prospects for Run 25 and
³⁰⁶ the EIC

³⁰⁷ Chapter 16

³⁰⁸ Remaining Questions

³⁰⁹ Chapter 17

³¹⁰ Implementation and application for
³¹¹ the remaining sPHENIX data

³¹² Bibliography

- ³¹³ ¹R. Atkin, “Review of jet reconstruction algorithms”, Journal of Physics: Conference Series **645**, 012008 (2015).
- ³¹⁴ ²G. P. Salam and G. Soyez, “A practical seedless infrared-safe cone jet algorithm”, Journal of High Energy Physics **2007**, 086–086 (2007).
- ³¹⁵ ³P. T. Komiske, E. M. Metodiev, and J. Thaler, “An operational definition of quark and gluon jets”, JHEP 11 (2018) 059 **2018**, 10.1007/jhep11(2018)059 (2018).
- ³¹⁶ ⁴L. M. Jones, “Tests for determining the parton ancestor of a hadron jet”, Physical Review D **39**, 2550–2560 (1989).
- ³¹⁷ ⁵Z. Fodor, “How to see the differences between quark and gluon jets”, Physical Review D **41**, 1726–1730 (1990).
- ³¹⁸ ⁶J. Gallicchio and M. D. Schwartz, “Pure samples of quark and gluon jets at the lhc”, Journal of High Energy Physics **2011**, 10.1007/jhep10(2011)103 (2011).
- ³¹⁹ ⁷D. Ferreira de Lima, P. Petrov, D. Soper, and M. Spannowsky, “Quark-gluon tagging with shower deconstruction: unearthing dark matter and higgs couplings”, Physical Review D **95**, 034001 (2017).
- ³²⁰ ⁸B. Bhattacherjee, S. Mukhopadhyay, M. M. Nojiri, Y. Sakaki, and B. R. Webber, “Quark-gluon discrimination in the search for gluino pair production at the lhc”, Journal of High Energy Physics **2017**, 10.1007/jhep01(2017)044 (2017).
- ³²¹ ⁹C. Adler, A. Denisov, E. Garcia, M. Murray, H. Stroebele, and S. White, “The rhic zero degree calorimeters”, Nuclear Instruments and Methods in Physics Research Section A: Accelerators, Spectrometers, Detectors and Associated Equipment **470**, 488–499 (2001).
- ³²² ¹⁰A. J. Larkoski, G. P. Salam, and J. Thaler, “Energy correlation functions for jet substructure”, Journal of High Energy Physics **2013**, 10.1007/jhep06(2013)108 (2013).
- ³²³ ¹¹Y. L. Dokshitzer, G. D. Leder, S. Moretti, and B. R. Webber, “Better jet clustering algorithms”, JHEP 9708:001,1997 **1997**, 001–001 (1997).